LETTERS

Botulinum neurotoxin B recognizes its protein receptor with high affinity and specificity

Rongsheng Jin[1,2], Andreas Rummel[3], Thomas Binz[4] & Axel T. Brunger[1,2]

Botulinum neurotoxins (BoNTs) are produced by *Clostridium botulinum* and cause the neuroparalytic syndrome of botulism. With a lethal dose of 1 ng kg^{-1}, they pose a biological hazard to humans and a serious potential bioweapon threat[1]. BoNTs bind with high specificity at neuromuscular junctions and they impair exocytosis of synaptic vesicles containing acetylcholine through specific proteolysis of SNAREs (soluble *N*-ethylmaleimide-sensitive fusion protein attachment protein receptors), which constitute part of the synaptic vesicle fusion machinery[2,3]. The molecular details of the toxin–cell recognition have been elusive. Here we report the structure of a BoNT in complex with its protein receptor: the receptor-binding domain of botulinum neurotoxin serotype B (BoNT/B) bound to the luminal domain of synaptotagmin II, determined at 2.15 Å resolution. On binding, a helix is induced in the luminal domain which binds to a saddle-shaped crevice on a distal tip of BoNT/B. This crevice is adjacent to the non-overlapping ganglioside-binding site of BoNT/B. Synaptotagmin II interacts with BoNT/B with nanomolar affinity, at both neutral and acidic endosomal pH. Biochemical and neuronal *ex vivo* studies of structure-based mutations indicate high specificity and affinity of the interaction, and high selectivity of BoNT/B among synaptotagmin I and II isoforms. Synergistic binding of both synaptotagmin and ganglioside imposes geometric restrictions on the initiation of BoNT/B translocation after endocytosis. Our results provide the basis for the rational development of preventive vaccines or inhibitors against these neurotoxins.

BoNTs are initially synthesized as a single-chain precursor protein. After cleavage by clostridial or tissue proteases, the active two-chain neurotoxin is fully capable of performing neurospecific binding, receptor-mediated endocytosis, endosomal translocation and target proteolysis[4]. Seven structurally and functionally related BoNTs exist, termed serotypes A to G, which are also related to tetanus neurotoxin (TeNT). The highly specific and strong binding of BoNTs with their cell-surface targets involves protein and ganglioside receptors that specifically localize to the neuronal plasma membrane[5]. At present, the only protein receptors to have been identified are synaptotagmin I (Syt-I) and synaptotagmin II (Syt-II) for both BoNT/B and BoNT/G, and synaptic vesicle protein SV2 (isoforms A, B and C) for BoNT/A[6–10]. Synaptotagmins are a family of transmembrane proteins that trigger Ca^{2+}-dependent neurotransmitter release. Syt-I and Syt-II are essential for synaptic transmission in neuromuscular junctions[11]. Both BoNT/B and BoNT/G exploit the luminal domains of Syt-I and Syt-II when they are temporarily exposed on the cell surface as a result of exocytosis, and the toxin–receptor complexes are then taken up by neurons through the recycling of secretory vesicles. Although ganglioside-binding sites have been identified for some BoNTs[12–14], the protein-receptor-binding sites have been unknown up to now.

The carboxy-terminal domain of the heavy chain of BoNT/B (referred to as H_CB) is responsible for specific binding with the luminal domains of Syt-I and Syt-II (ref. 6). To facilitate crystallization, we designed a fusion protein between H_CB (residues 858–1291) and Syt-II (8–61) (referred to as H_CB–Syt-II; Supplementary Fig. 1a). We validated the biological relevance of this strategy by a series of biochemical and cell-based studies. First, the fusion protein (H_CB–Syt-II) is monodisperse and monomeric in solution, thus ruling out the existence of a *trans*-complex that might complicate crystallization (Supplementary Fig. 1b). Second, a fusion construct between Syt-II (8–61) and full-length BoNT/B no longer interacts with free Syt-II (1–61) and its toxicity is decreased more than tenfold, suggesting that the Syt-II-binding site on BoNT/B is occupied in the fusion protein (Supplementary Fig. 1c, d). Third, structure-based mutagenesis studies based on H_CB or full-length BoNT/B confirmed the importance of interacting residues for binding affinity and toxicity (described below). Taken together, these data show that the covalently linked Syt-II forms a *cis*-complex with BoNT/B that faithfully represents the binary complex.

The structure of the complex between BoNT/B and Syt-II was determined to a minimum Bragg spacing of $d_{min} = 2.15$ Å by molecular replacement with the structure of H_CB (Protein Data Bank code 1Z0H) as the search model[15] (Supplementary Table 1). A difference electron-density map allowed unambiguous assignment of Syt-II residues 44–60, which are structured in the complex (Fig. 1a). This is consistent with the previous finding that residues 40–60 of Syt-II comprise a minimal BoNT/B-binding domain[9]. Residues 8–43 of Syt-II and the linker were not visible, probably as a result of conformational variability. The C terminus of H_CB is relatively close to the observed residue Glu 44 of Syt-II (about 41 Å; Fig. 1b), with the linker and Syt-II residues 8–43 providing a sufficient number of residues to connect the termini. Many possible paths between the termini are unobstructed by crystal packing, including those in a second structure we obtained in a different crystal form with a different packing arrangement at 3.2 Å resolution (not shown). We conclude that the linker does not affect the structure of the complex.

The luminal domain of Syt-II is unstructured in solution (Fig. 1d). On binding to H_CB, residues Glu 44 to Lys 60 become structured, with residues Phe 47 to Ile 58 forming an α-helix (Fig. 1a, b). Syt-II binds at the distal tip of the C-terminal domain of H_CB, in a saddle-shaped crevice on the surface formed by eight β-strands and four intervening loops. The strand that forms the base of the crevice is parallel to the Syt-II helix (Fig. 1b). The extensive intermolecular interface buries a solvent-accessible surface area of about 1,200 Å^2, involving mostly hydrophobic residues, with two pronounced pockets on the surface of H_CB (Fig. 2, and Supplementary Fig. 2). In addition, H_CB residues Lys 1113, Ser 1116 and Lys 1192 form salt

[1]Howard Hughes Medical Institute, [2]Departments of Molecular and Cellular Physiology, Neurology and Neurological Science, Structural Biology, and Stanford Synchrotron Radiation Laboratory, Stanford University, Stanford, California 94305, USA. [3]Institut für Toxikologie, [4]Institut für Biochemie, Medizinische Hochschule Hannover, Carl-Neuberg-Strasse 1, 30625 Hannover, Germany.

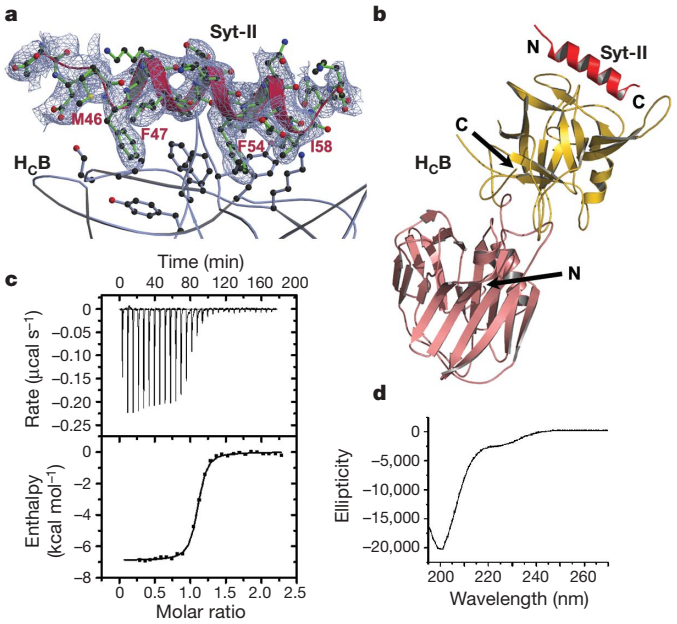

Figure 1 | Structure of the H_CB–Syt-II complex. **a**, σ_A-weighted $F_o - F_c$ electron-density map (contoured at 1.5σ) around Syt-II, overlaid with the final refined model (red and green, Syt-II; grey, H_CB). This map is model-bias free because it is calculated from the phases of the atomic model before the inclusion of the Syt-II peptide (using a lower-resolution diffraction data set to 2.6 Å). At this stage, the R_{work} and R_{free} values were 26.1% and 31.6%, respectively. **b**, Structure of the complex between H_CB (pink and gold) and Syt-II (red). **c**, Titration of GST–Syt-II (1–61) into H_CB by ITC at 20 °C and pH 7.5. $N = 1.1$; $K_a = 2.64 \times 10^7\ M^{-1}$; $\Delta H = -6{,}890$ cal mol^{-1}; $\Delta S = 10.4$ cal mol^{-1} K^{-1}. **d**, Far-ultraviolet circular dichroism spectra of the luminal domain of Syt-II (1–61).

bridges with residue Glu 57 of Syt-II. The structure of Syt-II-bound H_CB is very similar to that of the apo state with an overall root-mean-square deviation of 0.73 Å (ref. 15), with the notable exception of H_CB residues Glu 1191, Tyr 1183 and Phe 1204, which undergo significant rotamer changes on binding.

We measured the thermodynamics of the assembly of the H_CB–Syt-II complex in solution by using isothermal titration calorimetry (ITC). The tight binding of H_CB to Syt-II (average $K_d \approx 34$ nM) is stoichiometric (about 1:1), endothermic (average $\Delta H \approx -7.4$ kcal mol^{-1}; 1 cal ≈ 4.18 J) and entropy driven (average $\Delta S \approx 9.0$ cal mol^{-1} K^{-1}) (Fig. 1c, and Supplementary Table 2). The heat capacity (ΔC_p) for the H_CB–Syt-II interaction is about -326 cal mol^{-1} K^{-1}, which is consistent with a protein–protein interaction driven by the hydrophobic effect[16,17]. ITC titration at pH 5.7, mimicking the acidic endosomal environment, produced no change on assembly thermodynamics, indicating that the pH change associated with toxin internalization is unlikely to affect the binding of BoNT/B to its protein receptor (Supplementary Fig. 3b and Supplementary Table 2).

To study the specificity of the BoNT/B–Syt-II interaction, we performed structure-based mutagenesis studies both *in vitro* and in a neuronal assay. Point mutations were introduced in H_CB or Syt-II at or around the toxin–receptor interface. None of the H_CB single-site mutations caused an effect on protein folding and stability as verified by far-ultraviolet circular dichroism spectroscopy and thermal denaturation experiments. Most of the mutations in H_CB (V1118D, K1192E, F1194A, A1196K and F1204A) and in Syt-II (F47A, F54A, F55A and E57K) greatly decrease binding affinity (Fig. 3a, d), which is consistent with the significance of these residues for the H_CB–Syt-II interaction (Fig. 2). The relatively minor contribution of Met 46 and Leu 50 of Syt-II to the affinity is consistent with their locations at the periphery of the interface. The mutation of a residue located on the opposite side of the toxin–receptor interface, Syt-II-N59H, behaves similarly to the wild type. H_CB-S1199Y shows enhanced binding to Syt-II, perhaps as a result of a π-stacking interaction between Tyr 1199 of H_CB and Phe 47 of Syt-II.

We further examined the effects of the mutants in BoNT/B on physiological function—that is, toxicity—by using recombinant full-length single-chain BoNT/B applied at the mouse phrenic nerve[6,18] (Fig. 3b). The decrease in toxicity is marked (up to about 1,000-fold) for all mutations that reduce the interaction as shown by the pull-down experiments. The effect is comparable to or larger than that observed for mutations in the ganglioside-binding site[14]. It is remarkable that single-site mutants at the BoNT/B–Syt-II interface significantly attenuate the BoNT/B toxicity, suggesting that this protein–protein interface can be a target for the development of therapeutics to block the action of BoNT/B.

Syt-II alone is sufficient to mediate the binding and entry of BoNT/B into nerve cells, whereas Syt-I acts in a ganglioside-dependent manner[9], even though Syt-I and Syt-II are very similar in both primary sequence and function[19]. Furthermore, the dissociation constant (K_d) between H_CB and the luminal domain of Syt-I is at least two orders of magnitude larger than that between H_CB and the luminal domain of Syt-II (ITC data not shown). Residues of Syt that interact with H_CB are conserved in both Syt-I and Syt-II isoforms, except for Met 46, Phe 55 and Ile 58 (Fig. 3c). Because Met 46 of Syt-II contributes little to BoNT/B binding, we introduced Syt-II-like side chains

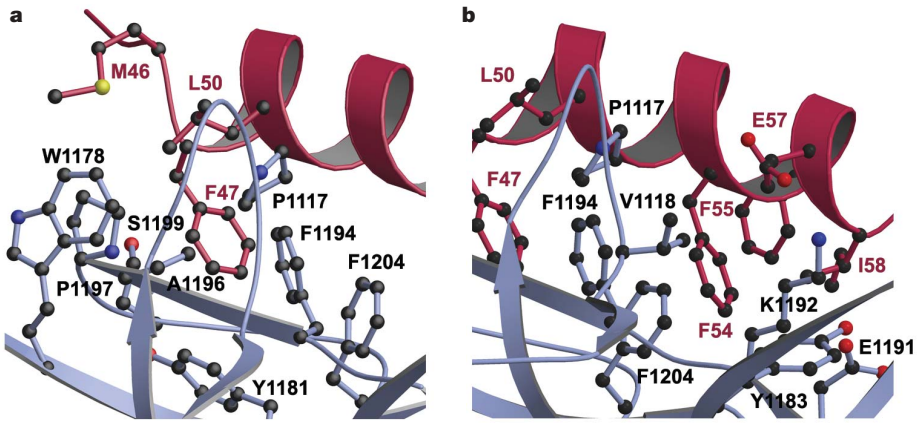

Figure 2 | The H_CB–Syt-II complex is stabilized by extensive intermolecular interactions involving two pronounced pockets on the H_CB surface. **a**, Pocket formed by H_CB residues Pro 1117, Trp 1178, Tyr 1181, Phe 1194, Ala 1196, Pro 1197 and Phe 1204, to which Syt-II residues Met 46, Phe 47 and Leu 50 bind. **b**, Pocket formed by H_CB residues Lys 1113, Ser 1116, Pro 1117, Val 1118, Tyr 1183, Glu 1191, Lys 1192, Phe 1194 and Phe 1204. Four Syt-II residues, Phe 54, Phe 55, Glu 57 and Ile 58 interact with this pocket. The complex of Syt-II (red) with H_CB (grey) is oriented similarly to that shown in Fig. 1a. Key residues are in ball-and-stick representation.

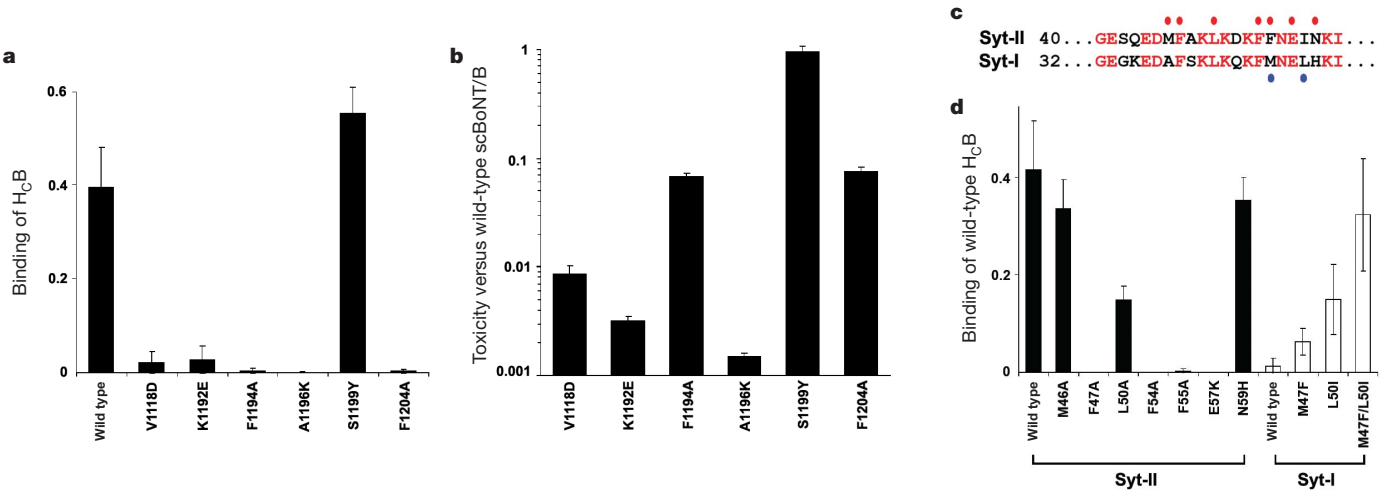

Figure 3 | Site-directed mutagenesis analysis of the toxin-receptor binding site in BoNT/B and in the luminal domains of Syt-I and Syt-II. **a**, Pull-down assay using GST–Syt-II wild type as bait in the presence of mixed ganglioside/Triton X-100 micelles shows drastically reduced binding of various H_CB single-site mutants. **b**, The corresponding single-site mutations in recombinant full-length single-chain BoNT/B confirm the drastic decrease in toxicity employing the mouse phrenic nerve as an *ex vivo* system. Results are plotted on a logarithmic scale. **c**, Sequence alignment of the membrane-proximal 22 amino acids of the luminal domain of rat Syt-I and Syt-II. The non-conserved residues are shown in black. Mutated residues of Syt-I and Syt-II are indicated with blue dots and red dots, respectively. **d**, Pull-down assay with H_CB wild-type and mutants of GST–Syt-II (1–61) (filled columns) and GST–Syt-I (1–53) (open columns) as bait in the presence of mixed ganglioside/Triton X-100 micelles shows the crucial role of Phe 47, Phe 54, Phe 55 and Glu 57 in Syt-II. Values in **a**, **b** and **d** are means ± s.d.

into Syt-I at the equivalent positions of residues 55 and 58. The double mutation (M47F/L50I) converts Syt-I into a Syt-II-like high-affinity receptor (Fig. 3d). The three BoNT/B residues (Glu 1191, Tyr 1183 and Phe 1204) that undergo rotamer changes on receptor binding are part of the pocket that interacts with these two Syt residues (Fig. 2b), indicating that this pocket of BoNT/B might have the key function in determining the protein-receptor-binding specificity.

Our results have implications for the function of BoNT/G, the closest homologue to BoNT/B, especially considering that the Syt-II-binding site is mostly conserved in BoNT/B and BoNT/G (Supplementary Fig. 4). BoNT/G also binds to the membrane-proximal region of Syt-I and Syt-II (ref. 6). Mutations of some of the BoNT/G residues that are equivalent to the Syt-interacting residues on BoNT/B significantly decrease the binding affinities between Syt-I and Syt-II and BoNT/G (ref. 20).

The two-receptor hypothesis for BoNTs was first proposed 20 years ago[21], although the relationship between these two receptors has been unclear. We now find that Syt-II and ganglioside occupy two adjacent but non-overlapping binding sites[12–14] (Fig. 4). The glucose of sialyllactose and the C terminus of the Syt-II luminal domain both point towards the membrane (Fig. 4). Sialyllactose (up to 12 μM) did not show a measurable effect on the binding between H_CB and the luminal domain of Syt-I as examined by ITC (data not shown). Deletion of the transmembrane domain of Syt-I abolishes ganglioside-dependent binding[22]. Thus, gangliosides do not enhance BoNT/B–Syt-I binding in an allosteric manner. However, the two receptors act synergistically in the context of the membrane because the dissociation constant between H_CB and the luminal domain of Syt in solution is more than 100-fold larger than that measured between BoNT/B and the full-length Syt (including the transmembrane region) in the presence of gangliosides and micelles[7]. Nevertheless, the interactions may be different for other members of the clostridial neurotoxin family because two carbohydrate-binding sites in the C-terminal part of the H_C fragment of TeNT are required for its function[23]. These different mechanisms of cell recognition probably cause their different targeting and sorting in peripheral neurons.

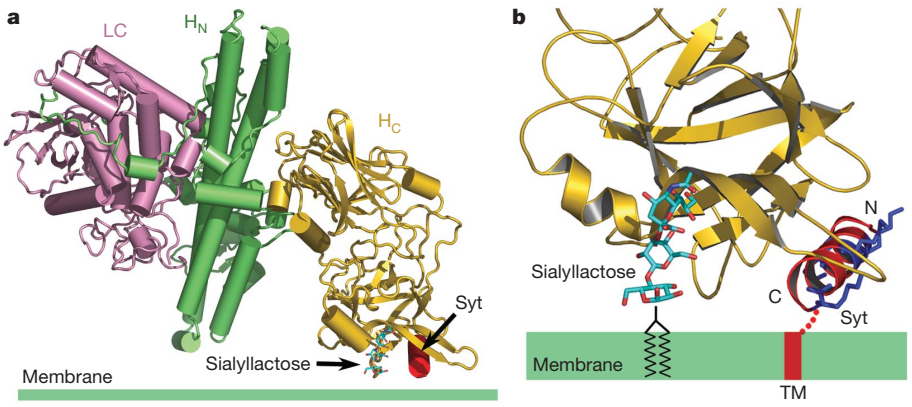

Figure 4 | Simultaneous binding with membrane-anchored Syt-II and ganglioside imposes geometric restrictions on how BoNT/B binds to the membrane surface. **a**, Proposed binding mode of BoNT/B on the membrane surface. The structure of a sialyllactose-bound BoNT/B (PDB code 1F31) was superimposed on the complex of H_CB–Syt-II by using the coordinates of the H_C fragment for the alignment. The light chain (LC), the N-terminal part of the heavy chain (H_N), and the C-terminal domain of the heavy chain (H_C) are shown in pink, green and gold, respectively. **b**, A close-up view of the proposed interface between BoNT/B and membrane. Four lysine residues that are conserved in Syt-I and Syt-II are coloured blue.

For BoNTs, a proper orientation on the membrane surface is important for efficient endocytosis and subsequent translocation of the light chain to the cytosol[24,25]. The simultaneous attachment of Syt and ganglioside imposes geometric restrictions on the position of BoNT/B with respect to the membrane surface (Fig. 4). The two mostly negatively charged molecular surfaces, which remain negatively charged even at luminal pH[26,27], further restrict the orientation of BoNT/B on the membrane surface (Supplementary Fig. 5a, b). In addition, four solvent-exposed lysine residues (Lys 49, Lys 51, Lys 53 and Lys 60) are conserved in both Syt-I and Syt-II (Fig. 3c) and might interact with the phospholipid headgroup region. BoNT/B probably adopts a similar binding mode on the membrane after the initiation of endosomal translocation, because the binding affinity between H_CB and the isolated Syt-II is independent of pH.

Given the safety concern about the currently used equine antitoxin therapy and the scarcity of the toxoid[1], effective binding inhibitors or vaccines are urgently needed against botulism. Our results are a step towards the development of safer vaccines, for example by using recombinant BoNT/B with structure-based mutations in the critical protein-receptor-binding site. The structure of the complex could also be used as a starting point for pharmacological inhibitor design.

METHODS

Detailed methods are provided in the Supplementary Information. In brief, the H_CB–Syt-II fusion protein was obtained from the H_C fragment of BoNT/B (H_CB, residues 858–1291) and the luminal domain of rat Syt-II (residues 8–61), connected by a 15-residue linker (PPTPGSAWSHPQFEK) including a Strep-tag (Supplementary Fig. 1a). Crystals were grown at 20 °C by vapour diffusion in two conditions: first, 13% polyethylene glycol (PEG) 6,000 and 0.1 M HEPES pH 7.0, and second, 0.8 M sodium citrate pH 6.5. The PEG condition yielded higher-quality crystals that diffracted to $d_{min} = 2.15$ Å. This crystal form adopts space group $P2_12_12_1$, with unit cell dimensions $a = 55.8$ Å, $b = 97.5$ Å, $c = 113.6$ Å, and one H_CB–Syt-II complex in the asymmetric unit. The structure of the H_CB–Syt-II complex was solved by molecular replacement with H_CB as the search model (PDB code 1Z0H) using Phaser[28]. The structure was built with the use of COOT[29] and refined to final $R_{work} = 19.9\%$ and $R_{free} = 24.5\%$ at 2.15 Å resolution with CNS[30]. The interactions between wild-type Syt-II and H_CB mutants, Syt-II mutants and wild-type H_CB, or Syt-I mutants and wild-type H_CB, were examined by a glutathione *S*-transferase (GST) pull-down assay. ITC experiments were conducted between H_CB and GST–Syt-II or Syt-II alone. Titrations were performed at different temperatures, protein concentrations and pH values. All H_CB mutations were further incorporated into full-length BoNT/B and the toxicities were determined by a mouse phrenic nerve toxicity assay[18]. The measured paralytic half-times were converted to toxicities against the corresponding wild-type BoNT/B.

Received 20 August; accepted 30 October 2006.
Published online 13 December 2006.

1. Arnon, S. S. *et al.* Botulinum toxin as a biological weapon: medical and public health management. *J. Am. Med. Assoc.* **285,** 1059–1070 (2001).
2. Schiavo, G. *et al.* Tetanus and botulinum-B neurotoxins block neurotransmitter release by proteolytic cleavage of synaptobrevin. *Nature* **359,** 832–835 (1992).
3. Chen, Y. A., Scales, S. J., Patel, S. M., Doung, Y. C. & Scheller, R. H. SNARE complex formation is triggered by Ca^{2+} and drives membrane fusion. *Cell* **97,** 165–174 (1999).
4. Montecucco, C. & Schiavo, G. Structure and function of tetanus and botulinum neurotoxins. *Q. Rev. Biophys.* **28,** 423–472 (1995).
5. Montecucco, C., Rossetto, O. & Schiavo, G. Presynaptic receptor arrays for clostridial neurotoxins. *Trends Microbiol.* **12,** 442–446 (2004).
6. Rummel, A., Karnath, T., Henke, T., Bigalke, H. & Binz, T. Synaptotagmins I and II act as nerve cell receptors for botulinum neurotoxin G. *J. Biol. Chem.* **279,** 30865–30870 (2004).
7. Nishiki, T. *et al.* The high-affinity binding of *Clostridium botulinum* type B neurotoxin to synaptotagmin II associated with gangliosides GT1b/GD1a. *FEBS Lett.* **378,** 253–257 (1996).
8. Dong, M. *et al.* SV2 is the protein receptor for botulinum neurotoxin A. *Science* **312,** 592–596 (2006).
9. Dong, M. *et al.* Synaptotagmins I and II mediate entry of botulinum neurotoxin B into cells. *J. Cell Biol.* **162,** 1293–1303 (2003).
10. Mahrhold, S., Rummel, A., Bigalke, H., Davletov, B. & Binz, T. The synaptic vesicle protein 2C mediates the uptake of botulinum neurotoxin A into phrenic nerves. *FEBS Lett.* **580,** 2011–2014 (2006).
11. Pang, Z. P. *et al.* Synaptotagmin-2 is essential for survival and contributes to Ca^{+2}-triggering of neurotransmitter release in central and neuromuscular synapses. *J. Neurosci.* (in the press).
12. Eswaramoorthy, S., Kumaran, D. & Swaminathan, S. Crystallographic evidence for doxorubicin binding to the receptor-binding site in *Clostridium botulinum* neurotoxin B. *Acta Crystallogr. D Biol. Crystallogr.* **57,** 1743–1746 (2001).
13. Swaminathan, S. & Eswaramoorthy, S. Structural analysis of the catalytic and binding sites of *Clostridium botulinum* neurotoxin B. *Nature Struct. Biol.* **7,** 693–699 (2000).
14. Rummel, A., Mahrhold, S., Bigalke, H. & Binz, T. The H_{CC}-domain of botulinum neurotoxins A and B exhibits a singular ganglioside binding site displaying serotype specific carbohydrate interaction. *Mol. Microbiol.* **51,** 631–643 (2004).
15. Jayaraman, S., Eswaramoorthy, S., Ahmed, S. A., Smith, L. A. & Swaminathan, S. N-terminal helix reorients in recombinant C-fragment of *Clostridium botulinum* type B. *Biochem. Biophys. Res. Commun.* **330,** 97–103 (2005).
16. Perozzo, R., Folkers, G. & Scapozza, L. Thermodynamics of protein–ligand interactions: history, presence, and future aspects. *J. Recept. Signal Transduct. Res.* **24,** 1–52 (2004).
17. Stites, W. E. Protein–protein interactions: interface structure, binding thermodynamics, and mutational analysis. *Chem. Rev.* **97,** 1233–1250 (1997).
18. Habermann, E., Dreyer, F. & Bigalke, H. Tetanus toxin blocks the neuromuscular transmission *in vitro* like botulinum A toxin. *Naunyn Schmiedebergs Arch. Pharmacol.* **311,** 33–40 (1980).
19. Südhof, T. C. Synaptotagmins: why so many? *J. Biol. Chem.* **277,** 7629–7632 (2002).
20. Rummel, A. *et al.* Identification of the protein receptor binding site of botulinum neurotoxins B and G proves the double receptor concept. *Proc. Natl Acad. Sci. USA* (in the press).
21. Montecucco, C. How do tetanus and botulinum neurotoxins bind to neuronal membranes? *Trends Biochem. Sci.* **11,** 314–317 (1986).
22. Kozaki, S., Kamata, Y., Watarai, S., Nishiki, T. & Mochida, S. Ganglioside GT1b as a complementary receptor component for *Clostridium botulinum* neurotoxins. *Microb. Pathog.* **25,** 91–99 (1998).
23. Rummel, A., Bade, S., Alves, J., Bigalke, H. & Binz, T. Two carbohydrate binding sites in the H_{CC}-domain of tetanus neurotoxin are required for toxicity. *J. Mol. Biol.* **326,** 835–847 (2003).
24. Koriazova, L. K. & Montal, M. Translocation of botulinum neurotoxin light chain protease through the heavy chain channel. *Nature Struct. Biol.* **10,** 13–18 (2003).
25. Hoch, D. H. *et al.* Channels formed by botulinum, tetanus, and diphtheria toxins in planar lipid bilayers: relevance to translocation of proteins across membranes. *Proc. Natl Acad. Sci. USA* **82,** 1692–1696 (1985).
26. Dolinsky, T. J., Nielsen, J. E., McCammon, J. A. & Baker, N. A. PDB2PQR: an automated pipeline for the setup of Poisson–Boltzmann electrostatics calculations. *Nucleic Acids Res.* **32,** W665–W667 (2004).
27. Li, H., Robertson, A. D. & Jensen, J. H. Very fast empirical prediction and rationalization of protein pK_a values. *Proteins* **61,** 704–721 (2005).
28. McCoy, A. J., Grosse-Kunstleve, R. W., Storoni, L. C. & Read, R. J. Likelihood-enhanced fast translation functions. *Acta Crystallogr. D* **61,** 458–464 (2005).
29. Emsley, P. & Cowtan, K. Coot: model-building tools for molecular graphics. *Acta Crystallogr. D* **60,** 2126–2132 (2004).
30. Brunger, A. T. *et al.* Crystallography & NMR system: A new software suite for macromolecular structure determination. *Acta Crystallogr. D* **54,** 905–921 (1998).

Supplementary Information is linked to the online version of the paper at www.nature.com/nature.

Acknowledgements We thank P. Adams and J. Zhou for critical reading of the manuscript, and the staff of beamlines 9-1 at the Stanford Synchrotron Radiation Laboratory (SSRL) and beam line 8.2.2 at the Advanced Light Source (ALS) for help during data collection; H. Bigalke for providing the mouse phrenic nerve facility; and T. Henke and C. Knorr for technical assistance. The SSRL is a national user facility operated by Stanford University on behalf of the US Department of Energy (Office of Basic Energy Sciences). The SSRL Structural Molecular Biology Program is supported by the Department of Energy (Office of Biological and Environmental Research), and by the National Institutes of Health (National Center for Research Resources, Biomedical Technology Program), and the National Institute of General Medical Sciences. The ALS is supported by the Office of Energy Research (Office of Basic Energy Sciences, Material Sciences Division) of the US Department of Energy at Lawrence Berkeley National Laboratory. Support by the Department of Defense and Defense Threat Reduction Agency (to A.T.B.) and by a Deutsche Forschungsgemeinschaft grant (to T.B.) is acknowledged.

Author Information The atomic coordinates and structure factors of the H_CB–Syt-II complex are deposited in the Protein Data Bank under accession code 2NM1. Reprints and permissions information is available at www.nature.com/reprints. The authors declare no competing financial interests. Correspondence and requests for materials should be addressed to A.T.B. (brunger@stanford.edu).